

Low Energy Gamma Ray Excess Confronting a Singlet Scalar Extended Inert Doublet Dark Matter Model

Amit Dutta Banik ¹, Debasish Majumdar ²

*Astroparticle Physics and Cosmology Division,
Saha Institute of Nuclear Physics,
1/AF Bidhannagar, Kolkata 700064, India*

Abstract

Recent study of gamma rays originating from the region of galactic centre has confirmed an anomalous γ -ray excess within the energy range 1-3 GeV. This can be explained as the consequence of pair annihilation of a 31-40 GeV dark matter into $b\bar{b}$ with thermal annihilation cross-section $\sigma v \sim 1.4 - 2.0 \times 10^{-26} \text{ cm}^3/\text{s}$. In this work we revisit the Inert Doublet Model (IDM) in order to explain this gamma ray excess. Taking the lightest inert particle (LIP) as a stable DM candidate we show that a 31-40 GeV dark matter derived from IDM will fail to satisfy experimental limits on dark matter direct detection cross-section obtained from ongoing direct detection experiments and is also inconsistent with LHC findings. We show that a singlet extended inert doublet model can easily explain the reported γ -ray excess which is as well in agreement with Higgs search results at LHC and other observed results like DM relic density and direct detection constraints.

¹email: amit.duttabanik@saha.ac.in

²email: debasish.majumdar@saha.ac.in

1 Introduction

Recent results from Femi-Lat data have confirmed the existence of GeV scale γ -ray excess which appear to be emerging from the region of galactic centre (GC) [1]-[10]. The annihilation of dark matter at the galactic centre may well be a cause for such excesses. The γ -ray peak in the energy range 1-3 GeV of gamma rays observed by Fermi-Lat to have come from the direction of galactic centre is addressed in a recent work by Dan Hooper et al [10]. In that work they show that a dark matter candidate within the mass range of 31-40 GeV primarily annihilating into $b\bar{b}$ or a 7-10 GeV dark matter primarily annihilating into $\tau\bar{\tau}$ [10]-[18] that eventually produce gamma, can well explain this observed phenomenon of excess gamma in 1-3 GeV energy range. Some works [7]-[8] even suggest a DM candidate with mass $61.8_{-4.9}^{+6.9}$ can also explain this observed excess when their annihilation cross-section $\langle\sigma v\rangle_{b\bar{b}}$ to $b\bar{b}$ is $\sim 3.30_{-0.49}^{+0.69} \times 10^{-26} \text{cm}^3/\text{s}$. Different particle physics models are studied and proposed in the literature in order to explain the anomalous excess of gamma ray in the energy range ~ 1 -3 GeV [19]-[28]. In this work we attempt to explore whether a dark matter candidate within the framework of the inert doublet model (IDM) [29]-[39] can explain this gamma ray excess in the gamma energy region of 1-3 GeV. In the inert doublet model, an additional scalar SU(2) doublet is added to the Standard Model (SM) which is assumed to develop no vacuum expectation value (VEV). An unbroken Z_2 symmetry ensures that the added scalar is stable and does not interact with the SM fermions (inert). The lightest stable inert particle (LIP) in this model can be a viable DM candidate. We show in this work that although LIP dark matter in IDM model may indeed provide a 31-40 GeV dark matter which satisfies observed DM relic density, but this candidate (of mass $\sim 31 - 40$ GeV) does not withstand the latest bounds from dark matter direct detection experiments as well as the LHC bound on $R_{\gamma\gamma}$. We then propose in this work, an extension of this IDM model whereby an additional singlet scalar is added to the IDM model mentioned above. This newly added scalar singlet acquires a non zero VEV and mixes up with the SM Higgs, thus provides an extra scalar boson and scalar resonance. The LIP dark matter candidate In this resulting extended IDM, as we show in this work, one can obtain an LIP dark matter candidate in the mass range of 31-40 GeV which sumultaneously satisfy the relic density bound from Planck experiment, direct detection experimental results and the bound on $R_{\gamma\gamma}$ from LHC experiment. We show that the calculation of gamma ray flux obtained from the annihilation of such a dark matter from the extended IDM model proposed in this work can explain the 1-3 GeV γ -ray excess observed by Fermi-LAT from GC region. The paper is organised as follows : In Section 2, we revisit the Inert Doublet Model of dark matter and show that for a 31-40 GeV DM, IDM cannot satisfy the constraints obtained from recent direct detection bounds on DM nucleon scattering cross-section σ_{SI} and is also inconsistent with the LHC constraints. In Section 3, we propose the singlet extended IDM and study the viability of the model to provide a DM candidate in the mass range 31-40 GeV that yields the right annihilation cross-section to $b\bar{b}$ final state ($\langle\sigma v\rangle_{b\bar{b}}$) required to explain the observed γ -ray excess in the energy range 1-3 GeV. We constrain the model

parameter space by various experimental results such as DM relic density obtained from Planck, DM-nucleon scattering cross-section bound from XENON, LUX experiments and bound on the SM-like scalar given by LHC. In Section 4, the gamma ray flux is calculated for the dark matter candidate in our proposed model and is compared with the observed results by Fermi-LAT. Finally we summarise the work in Section 5.

2 Dark Matter in Inert Doublet Model and Fermi-LAT observed gamma ray excess

IDM is a simple extension of SM of particle physics which includes an additional Higgs doublet that acquires no VEV. The added doublet do not interact with the SM sector due to imposition of a discrete Z_2 symmetry under which all the SM particles are even but the doublet is odd. The most general CP conserving potential for IDM is given as,

$$\begin{aligned}
V = & m_{11}^2 \Phi_H^\dagger \Phi_H + m_{22}^2 \Phi_I^\dagger \Phi_I + \lambda_1 (\Phi_H^\dagger \Phi_I)^2 + \lambda_2 (\Phi_I^\dagger \Phi_I)^2 + \lambda_3 (\Phi_H^\dagger \Phi_H) (\Phi_I^\dagger \Phi_I) \\
& + \lambda_4 (\Phi_I^\dagger \Phi_H) (\Phi_H^\dagger \Phi_I) + \frac{1}{2} \lambda_5 [(\Phi_I^\dagger \Phi_H)^2 + (\Phi_H^\dagger \Phi_I)^2],
\end{aligned} \tag{1}$$

where Φ_H is the SM Higgs doublet and Φ_I is the inert doublet assuming all the couplings (λ_i , $i = 1, 5$) in Eq. 1 are real. After spontaneous symmetry breaking (SSB), Φ_H generates a VEV $v = 246$ GeV whereas the inert doublet does not produce any VEV. The Z_2 symmetry remains unbroken. The doublets are given as

$$\Phi_H = \begin{pmatrix} \chi^+ \\ \frac{1}{\sqrt{2}}(v + h + i\chi^0) \end{pmatrix}, \quad \Phi_I = \begin{pmatrix} H^+ \\ \frac{1}{\sqrt{2}}(H_0 + iA_0) \end{pmatrix}, \tag{2}$$

where χ^+ and χ^0 are absorbed in W^\pm , Z after spontaneous symmetry breaking. After SSB, the masses of various scalar particles obtained are given as,

$$\begin{aligned}
m_h^2 &= 2\lambda_1 v^2 \\
m_{H^\pm}^2 &= m_{22}^2 + \lambda_3 \frac{v^2}{2} \\
m_{H_0}^2 &= m_{22}^2 + (\lambda_3 + \lambda_4 + \lambda_5) \frac{v^2}{2} \\
m_{A_0}^2 &= m_{22}^2 + (\lambda_3 + \lambda_4 - \lambda_5) \frac{v^2}{2}.
\end{aligned} \tag{3}$$

where $m_h = 125$ GeV, is the mass of newly found SM Higgs boson h , as observed by LHC experiments CMS [40] and ATLAS [41]. With $\lambda_5 < 0$, the lightest inert particle (LIP) H_0 is the stable DM candidate in the model. The potential described in Eq. 1 must be bounded from below and the corresponding vacuum stability conditions are given as,

$$\lambda_1, \lambda_2 > 0, \quad \lambda_3 + 2\sqrt{\lambda_1 \lambda_2} > 0, \quad \lambda_3 + \lambda_4 - |\lambda_5| + 2\sqrt{\lambda_1 \lambda_2} > 0. \tag{4}$$

Apart from the bounds obtained from vacuum stability, there are several other constraints on the model such as perturbative bounds requiring all the couplings Λ_i to be less than 4π . From LEP [42] experiment constraints of the Z boson decay width and charged scalar mass m_{H^\pm} , we have

$$\begin{aligned} m_{H_0} + m_{A_0} &> m_Z , \\ m_{H^\pm} &> 79.3 \text{ GeV}. \end{aligned} \quad (5)$$

Apart from the constraints presented in Eqs. 3-4, the present DM candidate H_0 must also satisfy the correct relic abundance of DM obtained from PLANCK [43]

$$\Omega_{\text{DM}} h^2 = 0.1199 \pm 0.0027 , \quad (6)$$

where h is the Hubble parameter in the unit of $100 \text{ km s}^{-1} \text{ Mpc}^{-1}$. Dark matter relic density is obtained by solving the Boltzmann equation for the DM species and is given as

$$\frac{dn_{H_0}}{dt} + 3Hn_{H_0} = -\langle\sigma v\rangle(n_{H_0}^2 - n_{H_0\text{eq}}^2) . \quad (7)$$

In Eq. 7 $\langle\sigma v\rangle$ is the total annihilation cross-section of the DM summing over all possible annihilation channels, n_{H_0} is the number density of dark matter particle H_0 and $n_{H_0\text{eq}}$ is the equilibrium number density of the same. The Hubble parameter is denoted as H in Eq. 7. For the case of low mass dark matter scenario ($m_{H_0} \leq m_W$, m_W is the mass of W boson), total annihilation cross-section of DM candidate H_0 to SM particles expressed as

$$\langle\sigma v_{H_0 H_0 \rightarrow f \bar{f}}\rangle = n_c \sum_f \frac{m_f^2}{\pi} \beta_f^3 \frac{(\lambda_L/2)^2}{(4m_{H_0}^2 - m_h^2)^2 + \Gamma_h^2 m_h^2} . \quad (8)$$

In Eq. 8 above, Γ_h is the total decay width of SM Higgs boson (including the contribution from invisible decay channel), m_f is the mass of the fermion species involved with $\beta_f = \sqrt{1 - \frac{m_f^2}{m_{H_0}^2}}$. The Higgs-DM coupling denoted as λ_L in Eq. 8 is of the form $\lambda_L = (\lambda_3 + \lambda_4 + \lambda_5)$ and n_c is the colour quantum number with $n_c = 3$ for quarks and $n_c = 1$ for leptons respectively. Invisible decay width of Higgs boson to DM particle as also the branching fraction Br_{inv} for such invisible decay is written as

$$\begin{aligned} \Gamma^{\text{inv}}(h \rightarrow H_0 H_0) &= \frac{\lambda_L^2 v^2}{64\pi m_h} \sqrt{1 - \frac{4m_{H_0}^2}{m_h^2}} , \\ \text{Br}_{\text{inv}} &= \frac{\Gamma^{\text{inv}}(h \rightarrow H_0 H_0)}{\Gamma_h} . \end{aligned} \quad (9)$$

DM relic density is then calculated by solving the Boltzmann equation expressed in Eq. 7, is given as

$$\Omega_{\text{DM}} h^2 = \frac{1.07 \times 10^9 x_F}{\sqrt{g_*} M_{\text{Pl}} \langle\sigma v\rangle} , \quad (10)$$

where $x_F = m_H/T_F$ is the freeze out or decoupling temperature of the DM species H_0 , M_{Pl} is the Planck mass ($M_{Pl} = 1.22 \times 10^{19}$ GeV) and g^* is the number of effective degrees of freedom. The quantity x_F (and subsequently the freeze out temperature T_f) can be obtained from the iterative solution to the equation

$$x_F = \ln \left(\frac{m_H}{2\pi^3} \sqrt{\frac{45 M_{Pl}^2}{2g^* x_F}} \langle \sigma v \rangle \right). \quad (11)$$

The relic density of the dark matter can be obtained using Eqs. 8-10 (and Eq. 11) with the constraints given in Eqs. 4-6. It is to be noted that in addition to the constraints mentioned above, the present DM candidate must also satisfy the DM direct detection experimental limits provided by the experiments like XENON [44], LUX [45]. The experiments provide the upper bound of dark matter scattering cross-sections for different dark matter masses. The spin independent direct dark matter-nucleon scattering cross-section for the LIP dark matter H_0 of mass M_{H_0} is expressed as

$$\sigma_{SI} = \frac{\lambda_L^2}{4\pi} \frac{1}{m_h^4} f^2 \frac{m_N^4}{(m_{H_0} + m_N)^2}, \quad (12)$$

where m_N is the mass of scattering nucleon and f is related to the matrix element of Higgs-

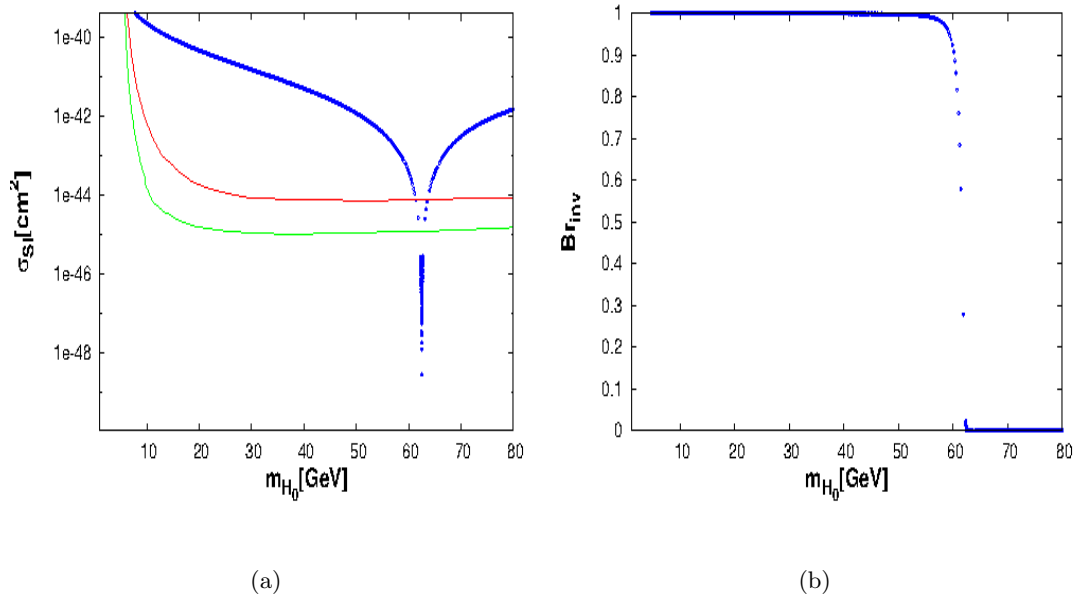


Figure 1: The left panel shows the $m_{H_0} - \sigma_{SI}$ space allowed by DM relic density obtained from PLANCK. The right panel presents the variation of invisible decay branching ratio Br_{inv} with DM mass m_{H_0} for the same.

nucleon coupling is taken to be $\simeq 0.3$ [46]. We further restrict the allowed model parameter space

by assuming the invisible decay branching ratio of SM Higgs $\text{Br}_{\text{inv}} < 20\%$ [47]. The branching ratio Br_{inv} is the ratio of the Higgs invisible decay width to the total Higgs decay width as discussed below. We compute, using Eq. 12 and with the constraints given in Eqs. 4-6, the LIP dark matter scattering cross-section, σ_{SI} for different values of LIP dark matter mass, m_{H_0} . It is therefore ensured that these calculations are performed for those LIP dark matter masses for which the relic density criterion (Eq. 6) is satisfied. The results are plotted in Fig. 1a (in $\sigma_{\text{SI}} - m_{H_0}$ plane). Superimposed on this plot in Fig. 1a are the the bounds obtained from XENON100 (red line) and LUX (green line) experimental results for comparison. It is clear from Fig. 1a that an LIP dark matter within the framework of IDM does not have a mass region in the range 31-40 GeV that satisfies the allowed bounds given by both the XENON100 and LUX experiments in $\sigma_{\text{SI}} - m_{H_0}$ plane. One may recall that the previous analysis to explain the Fermi-LAT γ -ray excess in the gamma ray energy range of 1 – 3 GeV [10] from the annihilation of dark matter at the galactic centre requires a dark matter candidate having mass in the range 31 – 40 GeV. We also compute the Higgs invisible decay branching ratio Br_{inv} for different m_{H_0} using Eq. 9 imposing the same constraints as above (Eqs. 4-6) and the results are plotted in Fig. 1b. It is also evident from Fig. 1b that the LIP mass (m_{H_0}) in the range 31-40 GeV does not satisfy the Br_{inv} limit of $\text{Br}_{\text{inv}} < 20\%$. Thus from both Fig 1a and Fig 1b, it can be concluded that an LIP dark matter in the inert doublet model cannot account for a viable dark matter candidate in the mass range of 31-40 GeV.

However, from Fig 1a and 1b, it is clear we have a viable dark matter candidate in the IDM framework in the region of Higgs resonance with mass ($m_{H_0} \simeq m_h/2$) that not only satisfies the relic density bound for dark matter but also is consistent with DM direct detection results and the bounds for Higgs invisible decay as well. Earlier model independent analysis [7]-[8] have reported that a dark matter with mass near Higgs resonance can produce the observed excess of γ -ray in the gamma energy range 1 – 3 GeV if the secondary γ -ray is produced out of the primary annihilation process $\text{DM DM} \rightarrow b\bar{b}$ with the annihilation cross-section $\langle\sigma v\rangle_{b\bar{b}} \sim 3.30_{-0.49}^{+0.69} \times 10^{-26} \text{ cm}^3/\text{s}$. However for IDM with mass $m_{H_0} \sim m_h/2$, the respective annihilation cross-section of LIP dark matter H_0 into $b\bar{b}$ channel is found to be result $\langle\sigma v\rangle_{b\bar{b}} \sim 1.7 \times 10^{-26}$ which is almost half the required annihilation cross-section. Hence the gamma-ray flux computed for this LIP dark matter (with $b\bar{b}$ to be the primary annihilation channel) does not comply with the observed excess in γ -ray.

Thus it is apparent that a viable dark matter candidate (mass $\sim m_h/2$) in the IDM model discussed so far where only an inert SU(2) doublet is added to SM, fails to explain the excess gamma ray in the energy range 1-3 GeV as observed by Fermi-LAT in the direction of galactic centre. Hence we consider a feasible extension of the model.

3 Inert Doublet Model with additional singlet scalar

We modify the IDM formalism given in Sect. 2 by adding another singlet scalar with the model. The resulting theory now includes an inert SU(2) doublet as before and an additional scalar singlet

added to the Standard Model. The newly added scalar singlet generates a VEV and is even under the discrete Z_2 symmetry. The LIP of the inert doublet is the dark matter candidate in this formalism too. We demonstrate that our proposed extended IDM provides a viable LIP dark matter candidate in the mass range of 31 – 40 GeV and the annihilation cross-section to $b\bar{b}$ channel for such a candidate can be calculated to be in the right ballpark required to explain the excess γ peak from GC seen by Fermi-LAT in 1-3 GeV energy range and is also consistent with the LHC constraint.

The most general potential for the model is

$$\begin{aligned}
V = & m_{11}^2 \Phi_H^\dagger \Phi_H + m_{22}^2 \Phi_I^\dagger \Phi_I + \frac{1}{2} m_s^2 S^2 + \lambda_1 (\Phi_H^\dagger \Phi_H)^2 + \lambda_2 (\Phi_I^\dagger \Phi_I)^2 + \lambda_3 (\Phi_H^\dagger \Phi_H) (\Phi_I^\dagger \Phi_I) \\
& + \lambda_4 (\Phi_I^\dagger \Phi_H) (\Phi_H^\dagger \Phi_I) + \frac{1}{2} \lambda_5 [(\Phi_I^\dagger \Phi_H)^2 + (\Phi_H^\dagger \Phi_I)^2] + \rho_1 (\Phi_H^\dagger \Phi_H) S + \rho'_1 (\Phi_I^\dagger \Phi_I) S \\
& + \rho_2 S^2 (\Phi_H^\dagger \Phi_H) + \rho'_2 S^2 (\Phi_I^\dagger \Phi_I) + \frac{1}{3} \rho_3 S^3 + \frac{1}{4} \rho_4 S^4,
\end{aligned} \tag{13}$$

where Φ_H and Φ_I are the same as in Eq. 1 with $S = s + v_s$, v_s being the VEV of the singlet scalar. All the parameters in Eq. 13 are assumed to be real. The newly added scalar singlet s mixes with the SM Higgs h resulting in two physical scalar bosons h_1 and h_2 and they are expressed as,

$$\begin{aligned}
h_1 &= h \cos \alpha - s \sin \alpha, \\
h_2 &= h \sin \alpha + s \cos \alpha,
\end{aligned} \tag{14}$$

where α is the angle of mixing. Minimising the potential in Eq. 13 we obtain the conditions,

$$\begin{aligned}
m_{11}^2 + \lambda_1 v^2 + \rho_1 v_s + \rho_2 v_s^2 &= 0, \\
m_s^2 + \rho_3 v_s + \rho_4 v_s^2 + \frac{\rho_1 v^2}{2v_s} + \rho_2 v^2 &= 0.
\end{aligned} \tag{15}$$

The mass terms for the scalars can be obtained as

$$\begin{aligned}
\mu_h^2 &= 2\lambda_1 v^2 \\
\mu_s^2 &= \rho_3 v_s + 2\rho_4 v_s^2 - \frac{\rho_1 v^2}{2v_s} \\
\mu_{h_s}^2 &= (\rho_1 + 2\rho_2 v_s) v \\
m_{H^\pm}^2 &= m_{22}^2 + \lambda_3 \frac{v^2}{2} + \rho'_1 v_s + \rho'_2 v_s^2 \\
m_{H_0}^2 &= m_{22}^2 + (\lambda_3 + \lambda_4 + \lambda_5) \frac{v^2}{2} + \rho'_1 v_s + \rho'_2 v_s^2 \\
m_{A_0}^2 &= m_{22}^2 + (\lambda_3 + \lambda_4 - \lambda_5) \frac{v^2}{2} + \rho'_1 v_s + \rho'_2 v_s^2.
\end{aligned} \tag{16}$$

As in Sect. 2, the lightest inert particle or LIP is H_0 when $\lambda_5 < 0$ and is the candidate for dark matter in this extended IDM formalism also.

Masses of physical scalars h_1 and h_2 derived using the mass matrix are,

$$m_{1,2}^2 = \frac{\mu_h^2 + \mu_s^2}{2} \pm \frac{\mu_h^2 - \mu_s^2}{2} \sqrt{1 + x^2}, \quad (17)$$

where $x = \frac{2\mu_{hs}^2}{(\mu_h^2 - \mu_s^2)}$. We consider h_2 with mass m_2 to be the SM-like Higgs boson having mass 125 GeV and we assume $m_2 > m_1$ where m_1 is the mass of the singlet scalar. Vacuum stability conditions for this singlet extended IDM are given as [48],

$$\begin{aligned} \lambda_1, \lambda_2, \rho_4 > 0, \quad \lambda_3 + 2\sqrt{\lambda_1\lambda_2} > 0, \quad \lambda_3 + \lambda_4 - |\lambda_5| + 2\sqrt{\lambda_1\lambda_2} > 0, \\ \rho_2 + \sqrt{\lambda_1\rho_4} > 0, \quad \rho'_2 + \sqrt{\lambda_2\rho_4} > 0, \\ & 2\rho_2\sqrt{\lambda_2} + 2\rho'_2\sqrt{\lambda_1} + \lambda_3\sqrt{\rho_4} \\ +2 \left(\sqrt{\lambda_1\lambda_2\rho_4} + \sqrt{\left(\lambda_3 + 2\sqrt{\lambda_1\lambda_2} \right) \left(\rho_2 + \sqrt{\lambda_1\rho_4} \right) \left(\rho'_2 + \sqrt{\lambda_2\rho_4} \right)} \right) > 0 \\ & 2\rho_2\sqrt{\lambda_2} + 2\rho'_2\sqrt{\lambda_1} + (\lambda_3 + \lambda_4 - \lambda_5)\sqrt{\rho_4} \\ +2 \left(\sqrt{\lambda_1\lambda_2\rho_4} + \sqrt{\left(\lambda_3 + \lambda_4 - \lambda_5 + 2\sqrt{\lambda_1\lambda_2} \right) \left(\rho_2 + \sqrt{\lambda_1\rho_4} \right) \left(\rho'_2 + \sqrt{\lambda_2\rho_4} \right)} \right) > 0. \end{aligned} \quad (18)$$

Imposing the vacuum stability conditions (Eq. 18) and applying the perturbative bounds and constraints from Eqs. 5-6 we solve the Boltzmann equation in Eq. 7. Note that, for the proposed extended IDM model, both the annihilation cross-section $\langle \sigma v_{H_0 H_0 \rightarrow f \bar{f}} \rangle$ and the invisible decay width $\Gamma_i^{\text{inv}}(h_i \rightarrow H_0 H_0)$ must be modified. The thermal averaged annihilation cross-section for the LIP dark matter in the present model is expressed as

$$\langle \sigma v_{H_0 H_0 \rightarrow f \bar{f}} \rangle = n_c \sum_f \frac{m_f^2}{\pi} \beta_f^3 \left| \frac{\lambda_{h_1 H_0 H_0} \cos \alpha}{4m_{H_0}^2 - m_1^2 + i\Gamma_1 m_1} + \frac{\lambda_{h_2 H_0 H_0} \sin \alpha}{4m_{H_0}^2 - m_2^2 + i\Gamma_2 m_2} \right|^2. \quad (19)$$

In Eq. 19 above, Γ_i ($i=1,2$) is the total decay width of h_i and the coupling $\lambda_{h_1 H_0 H_0}$, $\lambda_{h_2 H_0 H_0}$ are

$$\begin{aligned} \lambda_{h_1 H_0 H_0} v &= \left(\frac{\lambda_L}{2} c_\alpha - \frac{\lambda_s}{2} s_\alpha \right) v, \\ \lambda_{h_2 H_0 H_0} v &= \left(\frac{\lambda_L}{2} s_\alpha + \frac{\lambda_s}{2} c_\alpha \right) v \end{aligned} \quad (20)$$

with $\lambda_L = \lambda_3 + \lambda_4 + \lambda_5$ and $\lambda_s = \frac{\rho'_1 + 2\rho'_2 v_s}{v}$. Invisible decay width of h_1 and h_2 are given as

$$\Gamma_i^{\text{inv}}(h_i \rightarrow H_0 H_0) = \frac{\lambda_{h_i H_0 H_0}^2 v^2}{16\pi m_i} \sqrt{1 - \frac{4m_{H_0}^2}{m_i^2}}. \quad (21)$$

The LIP-nucleon spin independent (direct detection) cross-section in this singlet scalar extended IDM is modified as,

$$\sigma_{\text{SI}} = \frac{1}{\pi} \frac{m_N^4}{(m_{H_0} + m_N)^2} f^2 \left(\frac{\lambda_{h_1 H_0 H_0} \cos \alpha}{m_1^2} + \frac{\lambda_{h_2 H_0 H_0} \sin \alpha}{m_2^2} \right)^2. \quad (22)$$

As before, we restrict the model parameter space using the conditions from vacuum stability (Eq. 18), unitarity, LEP, DM relic density from PLANCK. In addition, we also take into account the modification of signal strength of SM Higgs (h_2) to any particular channel that may occur due to the mixing with other scalar (h_1). The signal strength to any specific channel is given as,

$$R = \frac{\sigma}{\sigma^{\text{SM}}} \frac{\text{Br}}{\text{Br}^{\text{SM}}} \quad (23)$$

where σ and σ^{SM} are the Higgs production cross-section in the present model and in SM respectively whereas Br and Br^{SM} are the respective branching ratios to any channel for the present model and SM. As the present model (extended IDM) involves two scalars h_1 and h_2 , signal strengths R_1 and R_2 for both the scalars are given as

$$R_1 = \frac{\sigma^1(pp \rightarrow h_1)}{\sigma^{\text{SM}}(pp \rightarrow h_1)} \frac{\text{Br}(h_1 \rightarrow xx)}{\text{Br}^{\text{SM}}(h_1 \rightarrow xx)}, \quad R_2 = \frac{\sigma^2(pp \rightarrow h_2)}{\sigma^{\text{SM}}(pp \rightarrow h_2)} \frac{\text{Br}(h_2 \rightarrow xx)}{\text{Br}^{\text{SM}}(h_2 \rightarrow xx)} \quad (24)$$

where xx is any SM final state with $\frac{\sigma^i}{\sigma^{\text{SM}}} = \cos^2 \alpha$ or $\sin^2 \alpha$ for $i = 1, 2$ respectively. Since h_2 is the SM-like scalar with mass $m_2 = 125$ GeV, we take $R_2 \geq 0.8$ [49] for SM-like scalar to satisfy LHC results. It is to be noted that some of the channels (γZ , $\gamma\gamma$) will suffer considerable changes due to the presence of inert charged scalars (H^\pm) addressed in [50, 51, 52, 53]. Effect of the charged scalars on those channels are also taken into account (see Appendix A). We put further bound on model parameter space from the experimental limits for Higgs to diphoton signal strength $R_{\gamma\gamma}$ given by ATLAS [54] and CMS [55]. Our calculation yields that for the allowed parameter space obtained from vacuum stability, relic density, LEP constraints as also with the condition $R_2 \geq 0.8$, $\text{Br}_{\text{inv}} \leq 0.2$, the Higgs to diphoton signal strength predicted by ATLAS is not favoured by the present model and hence we constrain the model with the experimental value of $R_{\gamma\gamma}$ only from CMS experiment. Taking all these constraints into account, we now compute the LIP dark matter (in extended IDM) scattering cross-sections σ_{SI} (Eq. 24) for the LIP masses (m_H) for two different mixing angles α given by $\cos \alpha = 9.0 \times 10^{-3}$ and 3.5×10^{-2} . The results for two chosen mixing angles are plotted in Fig. 2a and Fig. 2b respectively in $m_{H_0} - \sigma_{\text{SI}}$ parameter space. The calculations are performed with a chosen value $m_1 = 70$ GeV for the mass of the scalar singlet h_1 . Direct detection bounds from XENON100 and LUX are shown in Fig. 2a-b with the same color definitions used in Fig. 1a. It is clear from Fig. 2a-b that apart from obtaining a LIP dark matter of mass $\sim m_2/2$ (Higgs resonance) allowed by both XENON100 and LUX, we also obtain another allowed LIP mass of 35 GeV (due to the resonance of the added scalar involved in the model). Thus, the present modified inert doublet model produces a viable DM candidate with a mass of 35 GeV. Figs. 2a-b also indicate that the resonant behaviour is prominent for smaller values of mixing angle α . Increase in the mixing angle broadens the allowed $m_{H_0} - \sigma_{\text{SI}}$ parameter space with appreciable increase in DM-nucleon cross-section. In Fig. 2c-d we show the variation of R_2 with σ_{SI} where LIP dark matter mass $m_{H_0} = 35$ GeV is considered for the two mixing angles as chosen for Fig. 2a-b.

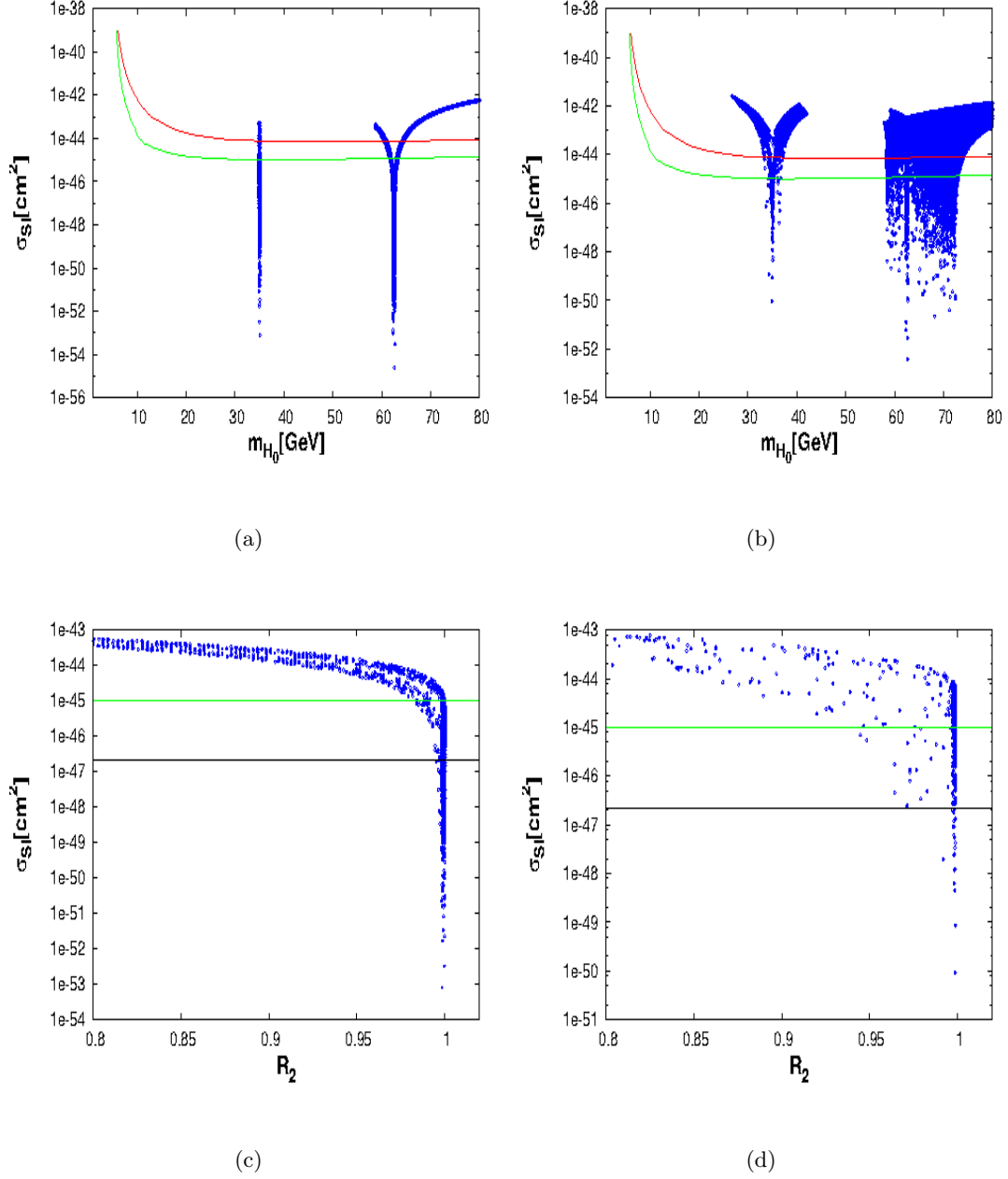


Figure 2: The upper panel shows the valid $m_{H_0} - \sigma_{SI}$ plane obtained for $m_2 = 70$ GeV with $\cos \alpha = 9.0 \times 10^{-3}$ and 3.5×10^{-2} . The lower panel shows the variation of signal strength R_2 with σ_{SI} for $m_{H_0} = 35$ GeV for the same.

Horizontal lines in green and black are the values of σ_{SI} as obtained from the allowed regions from LUX [45] and XENON1T [56] respectively for the dark matter mass of 35 GeV. Fig. 2c shows that

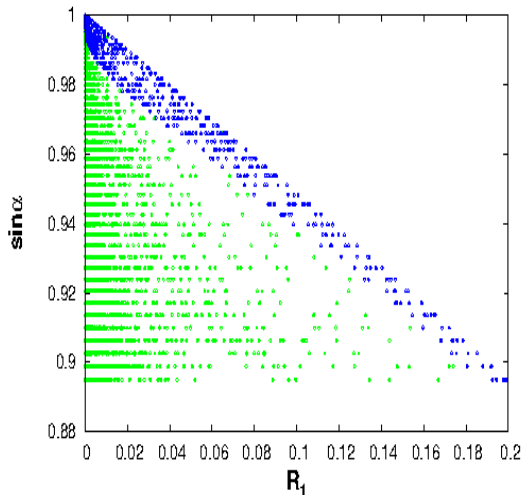


Figure 3: Allowed parameter space in $R_1 - \sin \alpha$ plane for $m_2 = 70$ GeV. Also shown in blue corresponds to the parameter space for $m_{H_0} = 35$ GeV.

as R_2 approaches to unity there is a sharp decrease in σ_{SI} . A similar conclusion also follows from the nature of Fig. 2d. Observation of Fig. 2c-d reveals that a 35 GeV DM satisfying relic density obtained from PLANCK and direct detection bounds from LUX and XENON1T does not affect the signal strength ($R_2 \sim 1$) of the SM Higgs observed in LHC. Fig. 2c-d clearly demonstrate that the presence of a low mass scalar is necessary in order to achieve a DM of mass ~ 35 GeV that (a) satisfy PLANCK relic density result, (b) agree with the latest dark matter direct detection experimental bounds and also (c) yields the experimental bound for Higgs invisible decay.

Since the model involves an additional scalar of low mass, yet undetected by LHC, the corresponding signal strength for that singlet like scalar must remain small compared to that of h_2 . In order to demonstrate this, we compute the signal strength R_1 (Eq. 24) for different values of the mixing angle α . In Fig. 3 we plot the results in $R_1 - \sin \alpha$ plane for low mass DM ($\leq m_W$). These results satisfy the conditions $R_2 \geq 0.8$ [49] and $\text{Br}_{\text{inv}} \leq 0.2$ [47] with $m_1 = 70$ GeV and also consistent with relic density reported by PLANCK. Scattered blue region in Fig. 3 corresponds to 35 GeV DM mass ($m_{H_0} = 35$ GeV) with $\langle \sigma v \rangle_{b\bar{b}} \sim (1.62 - 1.68) \times 10^{-26} \text{cm}^3/\text{s}$. We show latter in this in Sec. 4 that such a value for $\langle \sigma v \rangle_{b\bar{b}}$ in case of a dark matter mass of 35 GeV can indeed explain the Fermi-LAT observed excess of γ -ray in the energy range of 1-3 GeV. Variation of $\sin \alpha$ with R_1 in Fig. 3 depicts that for the parameter space constrained by different experimental and theoretical bounds, the value of the signal strength R_1 remains small (≤ 0.2). Therefore, non-observance of such a scalar by LHC is justified and can possibly be probed in future experiment.

m_1 in GeV	m_{H_0} in GeV	m_H^\pm in GeV	$\cos \alpha$	λ_L	λ_s	$\langle \sigma v \rangle_{b\bar{b}}$ in cm^3/s	σ_{SI} in cm^2
70.0	35.0	174.0	0.9×10^{-3}	-7.89e-05	-7.91e-02	1.66×10^{-26}	4.58×10^{-49}
		110.0	2.5×10^{-3}	7.87e-04	1.26e-02	1.65×10^{-26}	2.52×10^{-48}

Table 1: Benchmark points of singlet extended IDM with DM mass $m_{H_0} = 35$ GeV.

4 Calculation of gamma ray flux

In this section we calculate the gamma ray flux from the galactic centre due to the annihilation of 35 GeV dark matter in the extended IDM discussed in Sect.3. The gamma ray flux produced from DM annihilation in galactic centre is given by

$$\Phi = \frac{\langle \sigma v \rangle}{8\pi m_{DM}^2} \frac{dN}{dE_\gamma} J(\psi). \quad (25)$$

In Eq. 25, $\langle \sigma v \rangle$ is the annihilation cross-section, m_{DM} is the mass of the dark matter (m_{H_0} in the present scenario), $\frac{dN}{dE_\gamma}$ is the spectrum of photon produced due to DM annihilation. The factor $J(\psi)$ in Eq. 25 is the line of sight integral given as

$$J(\psi) = \int_{\text{los}} \rho^2(l, \psi) dl, \quad (26)$$

where ψ is angle between the line of sight of an observer at Earth at a distance ℓ from the GC and the direction from GC to Earth, l is the distance from line of sight. We use the generalised NFW [57] halo profile for the DM distribution $\rho(r)$ given by

$$\rho(r) = \rho_0 \frac{r/r_s^{-\gamma}}{1 + r/r_s^{3-\gamma}}. \quad (27)$$

In Eq. 27, $\rho_0 = 0.3 \text{ GeV cm}^{-3}$ is the local DM density at a distance 8.5 kpc from GC. For the present work we consider $r_s = 20$ kpc and $\gamma = 1.26$ [10]. For the calculation of gamma ray flux using Eqs. 25 - 27, we consider two values of mixing angles given by $\cos \alpha = 0.9 \times 10^{-3}$ and 2.5×10^{-2} for $m_{DM} = m_{H_0} = 35$ GeV. A chosen set of values for other parameters and the corresponding calculated values of $\langle \sigma v \rangle_{b\bar{b}}$ and σ_{SI} for each of these two mixing angles are tabulated in Table 1. The gamma ray flux is now calculated for the LIP dark matter in our model, in case of each of these two set of parameter values given in Table 1 and the results are plotted in Fig. 4. In Fig. 4 the green and blue lines correspond to the mixing angles given by $\cos \alpha = 0.9 \times 10^{-3}$ and $\cos \alpha = 2.5 \times 10^{-2}$ respectively. Also shown in Fig. 4, the data points for the observed γ -ray by Fermi-LAT for

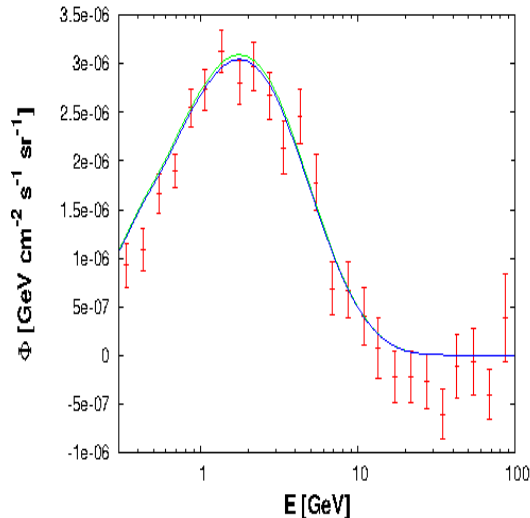


Figure 4: γ -ray flux obtained from the benchmark points in Table 1 and compared with the results from [10].

comparison. These data points are obtained from Ref. [10]. Fig. 4 clearly demonstrates that the viable LIP DM candidate in our model can very well explain the observed γ -ray flux and its excess in the 1-3 GeV energy range while remain consistent with the bounds from LHC and DM direct search experiments.

5 Summary

In this paper we have revisited the inert doublet model (IDM) of dark matter and test the viability of the model to provide a suitable explanation for the observed excess in low energy (1-3 GeV) γ -ray emission from GC assumed to have originated out of the annihilation of dark matter in the mass range 31-40 GeV DM, into $b\bar{b}$. We show that a dark matter candidate within mass range 31-40 GeV in IDM cannot satisfy the latest direct detection bounds on DM-nucleon cross-section predicted by experiments like LUX or XENON100 and also is inconsistent with the limits on Higgs invisible decay. Our calculation also yield that although IDM can provide a DM of mass $\sim m_h/2$ (m_h is the mass of SM Higgs) that is consistent with direct detection and invisible decay bounds but eventually fails to produce the exact value of $\langle\sigma v\rangle_{b\bar{b}}$ required to explain the excess emission of γ -ray. In order to comply with the observed γ emission results as obtained from Fermi-LAT in 1-3 GeV energy range, we extend the IDM with an additional singlet scalar and explore the viability of the model. The extension of IDM provides an additional scalar singlet that mixes with the SM-Higgs. We found that presence of a low mass singlet like scalar in the model can yield a 31-40 GeV DM that satisfy relic density bounds from PLANCK and direct detection cross-section constraints

from LUX or XENON experiments that and also yields the right DM annihilation cross-section $\langle\sigma v\rangle_{b\bar{b}}$ that would explain the observed excess in γ -ray. The weakly coupled singlet like scalar due to small mixing with SM-Higgs acquires a very small signal strength which is beyond the present LHC detection limit and can be probed in future collider experiments.

Appendix A

The inert charged scalar will contribute to Higgs decay channels like $\gamma\gamma$ and γZ through the charged scalar loop involved in the process. Decay widths of $h_i \rightarrow \gamma\gamma$, γZ ($i = 1, 2$) are given as

$$\begin{aligned}\Gamma(h_i \rightarrow \gamma\gamma) &= \frac{G_F \alpha_s^2 m_i^3}{128\sqrt{2}\pi^3} \left| c_i \left(\frac{4}{3} F_{1/2} \left(\frac{4m_t^2}{m_i^2} \right) + F_1 \left(\frac{4m_W^2}{m_i^2} \right) \right) + \frac{\lambda_{h_i H^+ H^-} v^2}{2m_{H^\pm}^2} F_0 \left(\frac{4m_{H^\pm}^2}{m_i^2} \right) \right|^2, \\ \Gamma(h_i \rightarrow \gamma Z) &= \frac{G_F^2 \alpha_s}{64\pi^4} m_W^2 m_i^3 \left(1 - \frac{m_Z^2}{m_i^2} \right)^3 \left| -2c_i \frac{1 - \frac{8}{3}s_W^2}{c_W} F'_{1/2} \left(\frac{4m_t^2}{m_i^2}, \frac{4m_t^2}{m_Z^2} \right) \right. \\ &\quad \left. - c_i F'_1 \left(\frac{4m_W^2}{m_i^2}, \frac{4m_W^2}{m_Z^2} \right) + \frac{\lambda_{h_i H^+ H^-} v^2 (1 - 2s_W^2)}{2m_{H^\pm}^2 c_W} I_1 \left(\frac{4m_{H^\pm}^2}{m_i^2}, \frac{4m_{H^\pm}^2}{m_Z^2} \right) \right|^2,\end{aligned}$$

where G_F is the Fermi constant and s_W (c_W) is $\sin\theta_W$ ($\cos\theta_W$) with θ_W representing the weak mixing angle. Factor c_i in the above is given as $\cos\alpha$ or $\sin\alpha$ for $i = 1, 2$. Couplings $\lambda_{h_1 H^+ H^-}$ and $\lambda_{h_2 H^+ H^-}$ in the expressions of decay widths are of the form

$$\begin{aligned}\lambda_{h_1 H^+ H^-} v &= (\lambda_3 c_\alpha - \lambda_s s_\alpha) v, \\ \lambda_{h_2 H^+ H^-} v &= (\lambda_3 s_\alpha + \lambda_s c_\alpha) v.\end{aligned}$$

Various loop factors corresponding to the $h_i \rightarrow \gamma\gamma$ process are expressed as [60, 61, 62],

$$\begin{aligned}F_{1/2}(\tau) &= 2\tau[1 + (1 - \tau)f(\tau)], \\ F_1(\tau) &= -[2 + 3\tau + 3\tau(2 - \tau)f(\tau)], \\ F_0(\tau) &= -\tau[1 - \tau f(\tau)],\end{aligned}$$

where the function $f(x)$ is given as

$$f(x) = \begin{cases} \arcsin^2\left(\frac{1}{\sqrt{x}}\right) & \text{for } x \geq 1, \\ -\frac{1}{4} \left[\log\left(\frac{1+\sqrt{1-x}}{1-\sqrt{1-x}}\right) - i\pi \right]^2 & \text{for } x < 1. \end{cases}$$

Similarly the loop factor for $h_i \rightarrow \gamma Z$ channel are [60, 61, 62]

$$\begin{aligned}F'_{1/2}(\tau, \lambda) &= I_1(\tau, \lambda) - I_2(\tau, \lambda), \\ F'_1(\tau, \lambda) &= c_W \left\{ 4 \left(3 - \frac{s_W^2}{c_W^2} \right) I_2(\tau, \lambda) + \left[\left(1 + \frac{2}{\tau} \right) \frac{s_W^2}{c_W^2} - \left(5 + \frac{2}{\tau} \right) \right] I_1(\tau, \lambda) \right\}.\end{aligned}$$

Expressions of the factors I_1 and I_2 are of the form

$$\begin{aligned} I_1(a, b) &= \frac{ab}{2(a-b)} + \frac{a^2b^2}{2(a-b)^2} [f(a) - f(b)] + \frac{a^2b}{(a-b)^2} [g(a) - g(b)], \\ I_2(a, b) &= -\frac{ab}{2(a-b)} [f(a) - f(b)]. \end{aligned}$$

where $f(x)$ is same as used in $h_i \rightarrow \gamma\gamma$ channel and $g(x)$ is given as

$$g(x) = \begin{cases} \sqrt{x-1} \arcsin \sqrt{\frac{1}{x}} & \text{for } x \geq 1, \\ \frac{\sqrt{1-x}}{2} \left(\log \frac{1+\sqrt{1-x}}{1-\sqrt{1-x}} - i\pi \right) & \text{for } x < 1. \end{cases}$$

References

- [1] L. Goodenough and D. Hooper; arXiv:0910.2998 [hep-ph].
- [2] D. Hooper and L. Goodenough, Phys. Lett. B **697**, 412 (2011).
- [3] A. Boyarsky, D. Malyshev and O. Ruchayskiy, Phys. Lett. B **705**, 165 (2011).
- [4] D. Hooper and T. Linden, Phys. Rev. D **84**, 123005 (2011).
- [5] K. N. Abazajian and M. Kaplinghat, Phys. Rev. D **86**, 083511 (2012).
- [6] C. Gordon and O. Macias, Phys. Rev. D **88**, 083521 (2013).
- [7] D. Hooper and T. R. Slatyer, Phys. Dark Univ. **2**, 118 (2013).
- [8] W. -C. Huang, A. Urbano and W. Xue; arXiv:1307.6862 [hep-ph].
- [9] K. N. Abazajian, N. Canac, S. Horiuchi and M. Kaplinghat; arXiv:1402.4090 [astro-ph.HE].
- [10] T. Daylan, D. P. Finkbeiner, D. Hooper, T. Linden, S. K. N. Portillo, N. L. Rodd and T. R. Slatyer; arXiv:1402.6703 [astro-ph.HE].
- [11] C. Boehm, M. J. Dolan, C. McCabe, M. Spannowsky, and C. J. Wallace; arXiv:1401.6458 [hep-ph].
- [12] T. Lacroix, C. Boehm and J. Silk; arXiv:1403.1987 [hep-ph].
- [13] A. Alves, S. Profumo, F. S. Queiroz and W. Shepherd; arXiv:1403.5027 [hep-ph].
- [14] A. Berlin, D. Hooper and S. D. McDermott; arXiv:1404.0022 [hep-ph].
- [15] P. Agrawal, B. Batell, D. Hooper and T. Lin; arXiv:1404.1373 [hep-ph].
- [16] E. Izaguirre, G. Krnjaic and B. Shuve; arXiv:1404.2018 [hep-ph].

- [17] S. Ipek, D. McKeen and A. E. Nelson; arXiv:1404.3716 [hep-ph].
- [18] K. Kong and J.-C. Park; arXiv:1404.3741 [hep-ph].
- [19] B. Kyae and J.-C. Park, Phys.Lett. B **732**, 373 (2014).
- [20] N. Okada and O. Seto, Phys.Rev. D **89**, 043525 (2014).
- [21] K. P. Modak, D. Majumdar, and S. Rakshit; arXiv:1312.7488 [hep-ph].
- [22] D. Cerdeno, M. Peiro and S. Robles; arXiv:1404.2572 [hep-ph].
- [23] C. Boehm, M. J. Dolan and C. McCabe; arXiv:1404.4977 [hep-ph].
- [24] P. Ko, W.-I. Park, and Y. Tang; arXiv:1404.5257 [hep-ph].
- [25] M. Abdullah et al.; arXiv:1404.6528 [hep-ph].
- [26] D. K. Ghosh, S. Mondal and I. Saha; arXiv:1405.0206 [hep-ph].
- [27] A. Martin, J. Shelton and J. Unwin; arXiv:1405.0272 [hep-ph].
- [28] T. basak, T. Mondal; arXiv:1405:4877 [hep-ph].
- [29] E. Ma, Phys. Rev. D **73**, 077301 (2006) [hep-ph/0601225].
- [30] L. Lopez Honorez, E. Nezri, J. F. Oliver and M. H. G. Tytgat, JCAP **0702**, 028 (2007) [hep-ph/0612275].
- [31] D. Majumdar and A. Ghosal, Mod. Phys. Lett. A **23**, 2011 (2008).
- [32] M. Gustafsson, E. Lundstrom, L. Bergstrom and J. Edsjo, Phys. Rev. Lett. **99**, 041301 (2007).
- [33] Q. -H. Cao, E. Ma and G. Rajasekaran, Phys. Rev. D **76**, 095011 (2007).
- [34] E. Lundstrom, M. Gustafsson and J. Edsjo, Phys. Rev. D **79**, 035013 (2009).
- [35] S. Andreas, M. H. G. Tytgat and Q. Swillens, JCAP **0904**, 004 (2009).
- [36] L. Lopez Honorez and C. E. Yaguna, JHEP **1009**, 046 (2010).
- [37] L. Lopez Honorez and C. E. Yaguna, JCAP **1101**, 002 (2011).
- [38] T. A. Chowdhury, M. Nemevsek, G. Senjanovic, and Y. Zhang, JCAP **1202**, 029 (2012).
- [39] D. Borah and J. M. Cline, Phys. Rev. D **86**, 055001 (2012).
- [40] S. Chatrchyan *et al.* [CMS Collaboration], Phys. Lett. B **716**, 30 (2012).

- [41] G. Aad *et al.* [ATLAS Collaboration], Phys. Lett. B **716**, 1 (2012).
- [42] J. Beringer *et al.* (Particle Data Group), Phys. Rev. D **86**, 010001 (2012).
- [43] P. Ade *et al.* [PLANCK Collaboration]; arXiv:1303.5076 [astro-ph.CO].
- [44] E. Aprile *et al.* [XENON100 Collaboration], Phys. Rev. Lett. **109**, 181301 (2012).
- [45] D. S. Akerib *et al.* [LUX Collaboration]; arXiv:1310.8214 [astro-ph.CO].
- [46] R. Barbieri, L. J. Hall and V. S. Rychkov, Phys. Rev. D **74**, 015007 (2006).
- [47] G. Belanger, B. Dumont, U. Ellwanger, J. Gunion, and S. Kraml, Phys.Lett. B723, 340 (2013).
- [48] K. Kannike, Eur. Phys. J. C **72**, 2093 (2012).
- [49] [ATLAS Collaboration], ATLAS-CONF-2012-162.
- [50] A. Arhrib, R. Benbrik, and N. Gaur, Phys. Rev. D **85**, 095021 (2012).
- [51] B. Swiezewska and M. Krawczyk, Phys. Rev. D **88**, 035019 (2013).
- [52] A. Goudelis, B. Herrmann and O. Stal, JHEP **1309**, 106 (2013).
- [53] A. D. Banik, D. Majumdar; arXiv:1404.5840 [hep-ph].
- [54] [ATLAS Collaboration], ATLAS-CONF-2013-012.
- [55] [CMS Collaboration], CMS-HIG-13-001.
- [56] E. Aprile [XENON1T Collaboration]; arXiv:1206.6288 [astro-ph.IM].
- [57] J. F. Navarro, C. S. Frenk, and S. D. White, Astrophys.J. **462**, 563 (1996).
- [58] T. Sjostrand, S. Mrenna, and P. Z. Skands, Comput.Phys.Commun. **178**, 852 (2008).
- [59] M. Cirelli, G. Corcella, A. Hektor, G. Hutsi, M. Kadastik, *et al.*, JCAP **1103**, 051 (2011).
- [60] J. F. Gunion, H. E. Haber, G. L. Kane, and S. Dawson, Front. Phys. **80**, 1 (2000).
- [61] A. Djouadi, Phys. Rept. **459**, 1 (2008).
- [62] A. Djouadi, Phys. Rept. **457**, 1 (2008).